IUST
Iran University of Science and Technology

Iranian Journal of Electrical and Electronic Engineering

Journal Homepage: ijeee.iust.ac.ir

Research Paper

A Reduction Method of Cogging Torque for Magnetic Gears

M. K. Rashid*, and A. M. Mohammed*(C.A.)

Abstract: Nowadays, magnetic gears (MGs) have become an alternative choice for mechanical gears because of their low maintenance, improved durability, indirect contact between inner and outer rotors, no lubrication, and high efficiency. Generally, although these advantages, MGs suffer from inherent issues, mainly the cogging torque. Therefore, cogging torque mitigation has become an active research area. This paper proposed a new cogging torque mitigation approach based on the radial slit of the ferromagnetic pole pieces of MGs. In this method, different numbers and positions of slits are applied. The best results are gained through an even number of slits which shows promising results of cogging torque mitigation on the inner rotor with a small mitigation in the mean torque on both rotors. This work is done by using Simcenter and MATLAB software packages. The inner rotor's cogging torque has mitigated to 81.9 %, while the outer rotor's cogging torque is increased only by 2.75 %.

Keywords: Magnetic Gear, Cogging Torque, Slitting Technique, 2D Finite Element Analysis.

1 Introduction

IN several applications, mechanical gears are extensively employed for power transmission and speed conversion. However, these gears suffer from many issues, mainly; contact friction and gear-tooth wear, noise, heat, and system failure. Therefore, magnetic gears (MGs) offer an alternative technology in order to overcome these issues [1].

In the early stage of MGs development, low-energy ferrite materials have been used. Therefore, the poor torque density can only transfer a low amount of torque. Recently, high-energy magnets have been effectively utilized to increase the power density and allow higher torque to be transmitted [2].

Iranian Journal of Electrical and Electronic Engineering, 2023.
Paper first received 15 Dec 2022, revised 06 Feb 2023, and accepted 10 Feb 2023.
*The authors are with the Department of Electrical and Electronics Engineering, University of Technology, Baghdad, Iraq
E-mails: muhammed.k.alrikabi@uotechnology.edu.iq and ahmed.m.mohammed@uotechnology.edu.iq.
Corresponding Author: A. M. Mohammed.
https://doi.org/10.22068/IJEEE.19.2.2752.

Generally, PM machines suffer from torque ripple related to their design construction. This ripple causes a mechanical vibration and a control difficulty in position and speed; hence, functionality problems in the drive system occur. Many factors contribute to the torque ripple; because of the configuration of stator teeth and rotor PM poles, the cogging torque which is the most significant factor is appeared [3]. Regarding MGs, the main challenge is to mitigate the cogging torque, so more effort is needed to cover this issue.

In the literature, a number of approaches for alleviating the cogging torque have already been proposed. Magnet shaping and sizing, teeth pairing, magnet angle, slot pairing, slicing, and magnet shifting are proposed in [3-9]. In [10], a simple method in which irregular magnet shift has been applied for the surface-mounted PM rotor of brushless direct current (BLDC) machines. Cogging torque could also be minimized by using skewing techniques [11], pole-piece notches[12-14], irregular slot openings [15], and selecting the proper magnet poles-pairing [16]. Skewing methods are ineffective for the segmented stator core machines because the segmentation and stator

asymmetries generate additional low-order harmonics [11, 17, 18]. In [19], a semi-analytical technique based upon the shift of slot-opening is provided to reduce the additional low-order harmonics, which tend to mitigate the cogging torque by 85%. However, this approach is restricted to segments of the stator core with doubled slots.

All the up mentioned methods contribute to enhancing the performance of PM machines. However, the manufacturing process and cost play a significant role in most industrial developments. In this research, a new and simple approach for mitigating the cogging torque is proposed keeping the MG rotors unaltered. This proposed method depends on the slitting technique by making radial slits in the ferromagnetic pole pieces at different positions; therefore, the slots between the pole pieces are reduced with the cost of small mitigation in the average torque.

In this work, the MG of [20] has been selected, which is taken as a case of study. In this model, the cogging torque appears on both rotors, and the largest value appears in the inner rotor. Consequently, the largest value of cogging torque will be seen by the input source and hence, affects the driver performance. At the same time, the MG's outer rotor is coupled to the output load of a mechanical rotating driving part, such as vehicle wheels, where the cogging torque is vanished due to their large inertia.

The finite element method in two dimensions (2D-FEM) technique is used for modelling and analyzing the proposed method using Simcenter software linked with MATLAB software for facilitating the evaluation of the method and optimization process. The results are contrasted with the previously designed model [20]. According to the selected model, the outer rotor's cogging torque is very small; hence, the new approach has been proposed to mitigate the high value of cogging torque which appears in the inner rotor. The method could be proposed to alleviate the cogging torque of the two rotors, on the other hand, the low value of the outer cogging torque has not been taken into account.

2 Structures and Working Principle

2.1 Principle of Operation

In general, MG is formed from a high-speed rotor (HSR) which represents the inner rotor, a low-speed rotor (LSR) which represents the outer rotor, and ferromagnetic pole pieces (n_s) which represents in this work the stationary part. The principle of operation is based upon the air gap flux's modulation. The harmonics flux density distribution created by modulating the magnetic field resulting from the outer rotor PMs through the pole pieces will travel to the inner air gap adjoining the HSR, so the PMs of the inner rotor's pole-pairs should be similar to the pole-pairs of the harmonics flux density for synchronism. Fig. 1 shows the general structure of the selected MG of [20].

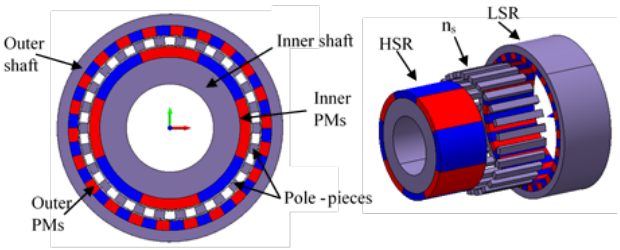

Fig. 1 The general structure of the MG.

The pole-pairs number of the component of fundamental harmonics flux density (p_{sl}) resulting from the outer rotor PMs and modulated through the pole pieces at the air gap adjoining the HSR, is given in Eq. (1) and the component of fundamental harmonics of flux density generated by PMs of the HSR (p_{sh}) is given in Eq. (2). The revolving velocity of the harmonics flux density adjoining the HSR (ω_{sl}) is given in Eq. (3).

$$p_{sl} = |p_l - n_s| \tag{1}$$

$$p_{sh} = |p_h - n_s| \tag{2}$$

$$\omega_{sl} = \frac{p_l}{p_l - n_s} * \omega_l - \frac{n_s}{p_l - n_s}\omega_s \tag{3}$$

where, p_l, p_h, ω_l and ω_s are the pole-pairs of the LSR PMs, HSR PMs, the revolving velocity of the LSR, and the revolving velocity of the pole pieces, respectively. Since the pole pieces are stationary, then $\omega_s = 0$. For transmitting the power between the two rotors and for synchronism, the inner rotor pole-pairs p_h must be equal to p_{sl}, as well, the outer rotor pole-pairs $p_l = p_{sh}$ as a result, the pole pieces number can be found as in Eq. (4). The revolving velocities of the HSR (ω_h) and LSR are in Eq. (5).

$$n_s = p_h + p_l \tag{4}$$

$$\omega_h = -\frac{p_l}{p_h} * \omega_l \rightarrow \frac{\omega_h}{\omega_l} = -\frac{p_l}{p_h} \tag{5}$$

$$G_r = -\frac{p_l}{p_h} \tag{6}$$

where G_r is the gear transmission ratio having a minus sign which means that the inner rotor's velocity is opposite to the outer rotor's velocity. The net power equation at steady-state ignoring the

power losses is shown in Eq. (7) and (G_r) is given in Eq. (8):

$$\omega_h T_h + \omega_l T_l + \omega_s T_s = 0 \quad (7)$$

$$\frac{T_l}{T_h} = \frac{\omega_h}{\omega_l} = -\frac{p_l}{p_h} = G_r \quad (8)$$

where T_h, T_l and T_s are the torque of the HSR, LSR, and pole pieces, respectively.

2.2 Cogging Torque Definition

For PM machines, cogging torque (T_{cog}) is a result of the interaction of pole pieces and PMs poles; it is a parasitic torque and is affected by the air gap flux (φ_g) and reluctance ($\Re$) variations, and can be expressed as in Eq. (9) [21]:

$$T_{cog} = -\frac{1}{2}\varphi_g^2 \frac{d\Re}{d\vartheta} \quad (9)$$

where ϑ and $\frac{d\Re}{d\vartheta}$ are the rotor's angular position and the change rate of the reluctance concerning the rotor position, respectively. Fig. 2 illustrates a schematic diagram of a PM pole of the rotor and the pole pieces group of the stator, with the cogging torque waveform. If the PM pole is centered at position (a), the reluctance, through which the flux passes, is maximum and $\frac{d\Re}{d\vartheta}$ is zero. In this position, the T_{cog} is zero and considered as a critical position where the PM pole tend to move to the right or left according to the nearest tooth. If the PM pole is moved to the right and centered at (b), the reluctance from position (a) to (b) has a negative slope where $\frac{d\Re}{d\vartheta}$ is negative, and the resultant T_{cog} as in Eq. (9), has a maximum positive value. Continuously from position (b) to (c), the reluctance is slightly decreased; in this stage the T_{cog} is lowered but still has a positive value. When the PM pole is centered at position (c), then the reluctance is minimum, and this is called the stable position where the T_{cog} is zero. Similarly, from position (c) to (d), the reluctance is slightly increased, creating a positive slope for which $\frac{d\Re}{d\vartheta}$ is positive and the T_{cog} has a maximum negative value at position (d). Furthermore, from position (d) to (e), the reluctance is increased; in this stage, the T_{cog} is lowered with a negative value and zero at position (e) for which maximum reluctance is obtained. The result is a full cycle cogging torque waveform.

The selected MG parameters are listed in Table 1 [20]. For the HSR, the least common multiple $LCM(2p_h, n_s)$ is equal to 104, this indicates the fundamental component of the HSR cogging torque. While for the LSR, the $LCM(2p_l, n_s)$ is equal to 572, which indicates the fundamental component of the LSR cogging torque.

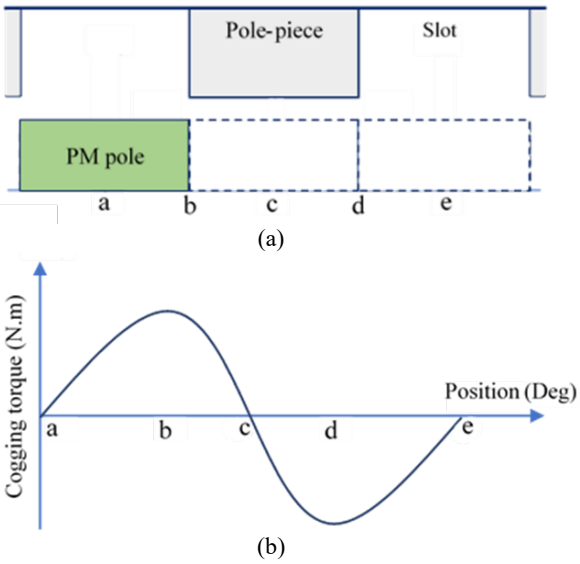

Fig. 2 Cogging torque phenomenon: a) pole pieces and PM pole arrangement and b) cogging torque waveform.

Table 1 Geometric parameters of the MG.

Description	Value
Pole-pairs of HSR PMs	4
Pole-pairs of LSR PMs	22
Pole-pieces number	26
Air gap length	1 mm
The pole-pieces radial thickness	5 mm
Axial length	50 mm
The back iron radius of inner rotor	43.5 mm
The back iron thickness of HSR	16.5 mm
The radial thickness of HSR PMs	6.5 mm
The back iron radius of outer rotor	70 mm
The back iron thickness of outer rotor	7 mm
The radial thickness of LSR PMs	6 mm
Remanence flux density	1.26 T

3 Proposed Technique of Cogging Torque Reduction

This paper proposes a new approach to mitigate the cogging torque depending on the slitting technique. The principle of this method is based on narrowing the slots of the pole pieces by making radial slits through them. The essential factor is the selection of the number of slits n, slit width d, and the slit angle α with respect to the radial line bisecting the pole piece, i.e., slitting position. Fig. 3 shows the proposed slitting method applied to the selected MG [20] with different numbers and positions of slits. Fig. 4 compares the waveforms of cogging of the slitted pole pieces with the pole pieces of the original model.

It can be noted that both the number and position of slits directly affect the reference axis of

the cogging torque, where this reference must be at zero position.

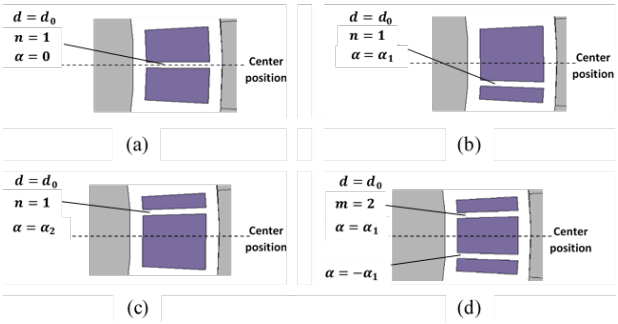

Fig. 3 The sectional view of several slitting types of pole pieces.

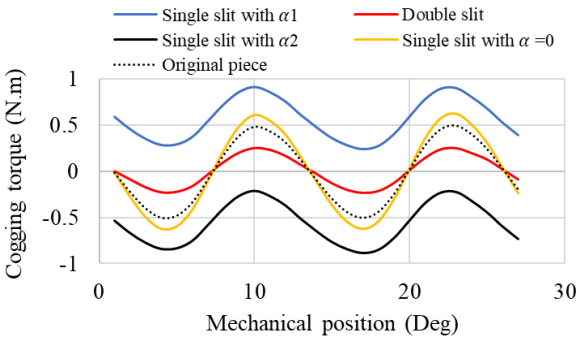

Fig. 4 Cogging torque waveforms.

In case (a), the slit bisects the pole pieces, so that, the stored energy is equally distributed between each half of the pole pieces. Therefore, the mean value of cogging torque waveform is zero, viz. zero reference; but the peak value is large because a small distance d_o separates the halved pieces, and the pieces volume is equal, hence, sharing the same stored energy. While in case (b), the slit position is diverted from the center position, so that, there are asymmetric volumes of the partitioned pole pieces. Therefore, the piece of small volume stores less energy than the large piece volume, so the reference position of the overall cogging torque tends to be positive where the center of the large piece volume is positive with respect to the center position. The principle is the same as for (c), except that there is a negative reference position for the cogging torque waveform. In case (d), the pole pieces are divided into three parts; the upper piece stores small energy of a positive reference, the middle piece stores energy of a zero reference, and the lower piece stores the same energy as the upper piece but with a negative reference through which the positive reference of the upper piece is canceled. Therefore, the resultant is a stored energy with zero reference. The optimal slit of the four types is verified in case (d), through which a reduced cogging torque is obtained.

From the up mentioned types, some of the constraints should be considered:

1. The slits number n must be even 2, 4, 6, **…**
2. The asymmetric slit should be avoided, considering the symmetric slit always.
3. The slit must be radial or parallel to the flux line direction. The inclined or circular slit may oppose the magnetic flux lines.

For the proposed model, the two-slits method (case (d)) has been chosen for reducing the cogging torque.

4 Results and Discussion

4.1 Magnetic Flux Density

For the selected MG, to verify the reliability of the equations mentioned in section 2, the superposition theorem is applied to analyze the harmonics of flux density for the magnets of both rotors. Analyzing the model by 2D static solver gives the flux density variations and the corresponding fast Fourier transform (FFT) spectra in the air gaps adjacent to both rotors over $360^o mech$. First, by disabling the HSR magnets and only the LSR magnets are existed in the model. The analysis of this configuration is shown in Fig. 5; it can be seen that in Fig. 5b, the order of the fundamental flux density in the air gap adjoining the LSR is 22, which is similar to 22 pole-pairs of the LSR magnets; in addition, in Fig. 5d, the order of the component of fundamental harmonics of flux density at the air gap adjoining the HSR is 4 which represents the quotient of the fundamental component of LSR and the gear ratio (5.5). In other words, this analysis agrees with Eq. (1); therefore, the pole-pairs of HSR magnets should be similar to p_{sl} for synchronism and correct operation of the MG. Second, disabling the LSR magnets and only the HSR magnets exist in the model; the analysis of this configuration is shown in Fig. 6, where the order of the fundamental flux density at the air gap adjoining the HSR is 4, as shown in Fig. 6b, which is identical to pole-pairs of the HSR magnets, while the order of the component of fundamental harmonics of flux density at the air gap adjoining the LSR is 22, as shown in Fig. 6d, which is similar to pole-pairs of the HSR magnets multiplied by 5.5, where this has the agreement with Eq. (2), and the pole-pairs of LSR magnets must be similar to p_{sh}. Finally, the flux density excited by the PMs of both rotors is analyzed. Fig. 7 compares the radial flux density variations of the two models.

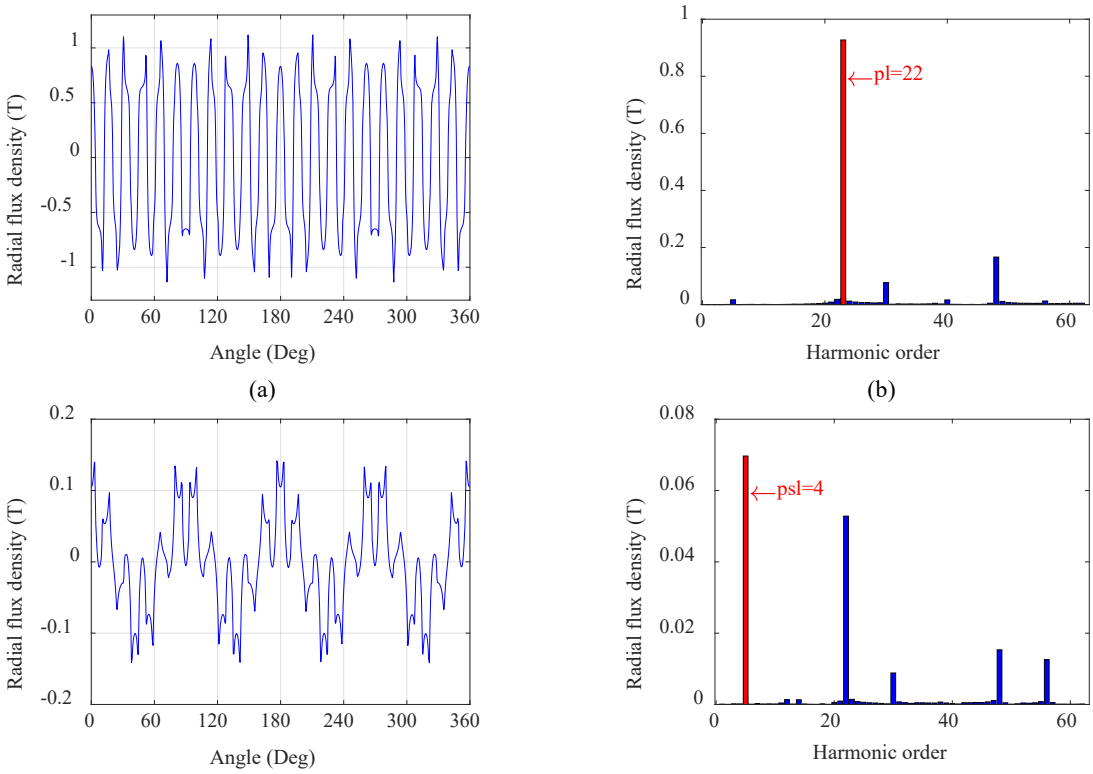

Fig. 5 Flux density variation and its FFT spectra considering the LSR magnets: a) and b) Air gap adjoining the LSR, c) and d) Air gap adjoining the HSR.

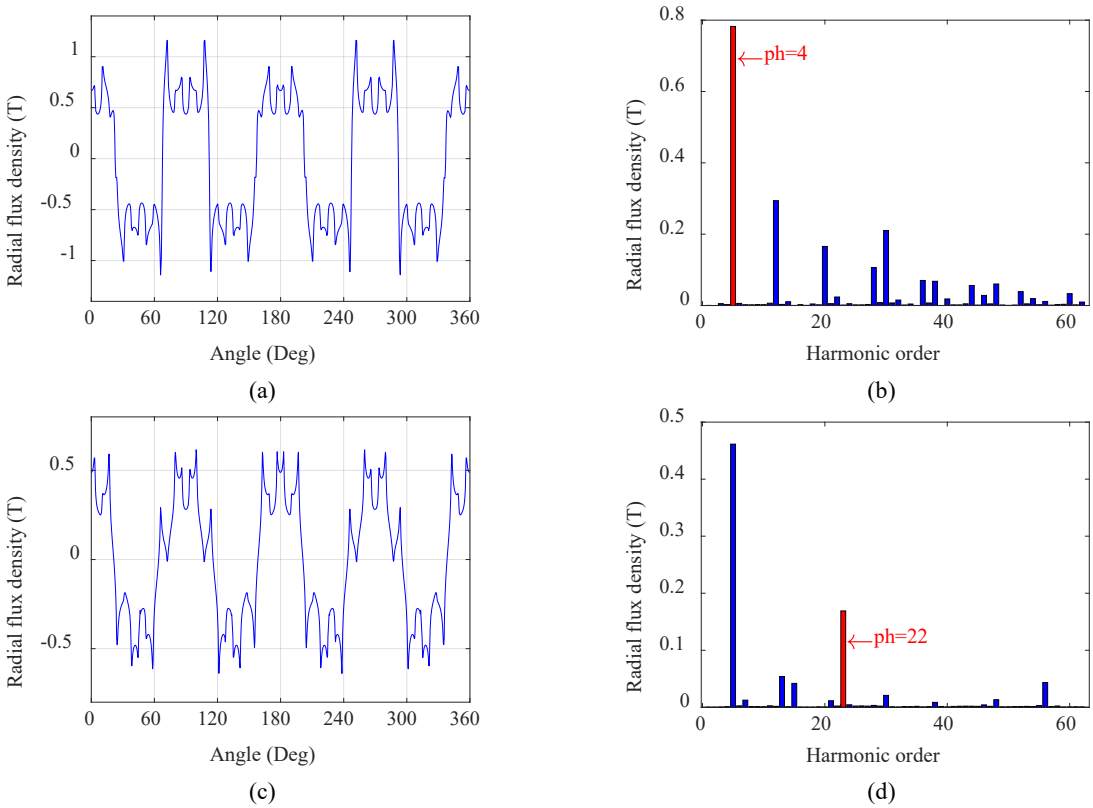

Fig. 6 Flux density variation and its FFT spectra considering the HSR magnets: a) and b) Air gap adjoining the HSR, c) and d) Air gap adjoining the LSR.

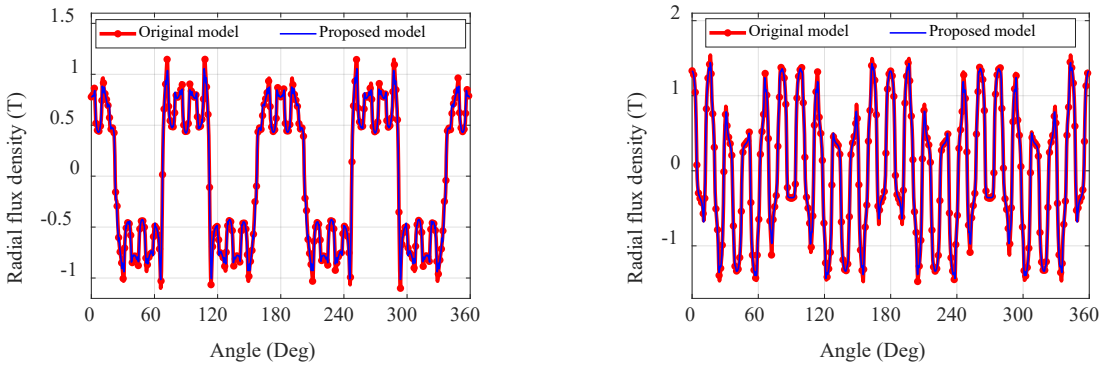

Fig. 7 Flux density variation considering the magnets of both rotors: a) Air gap adjoining the HSR and b) Air gap adjoining the LSR.

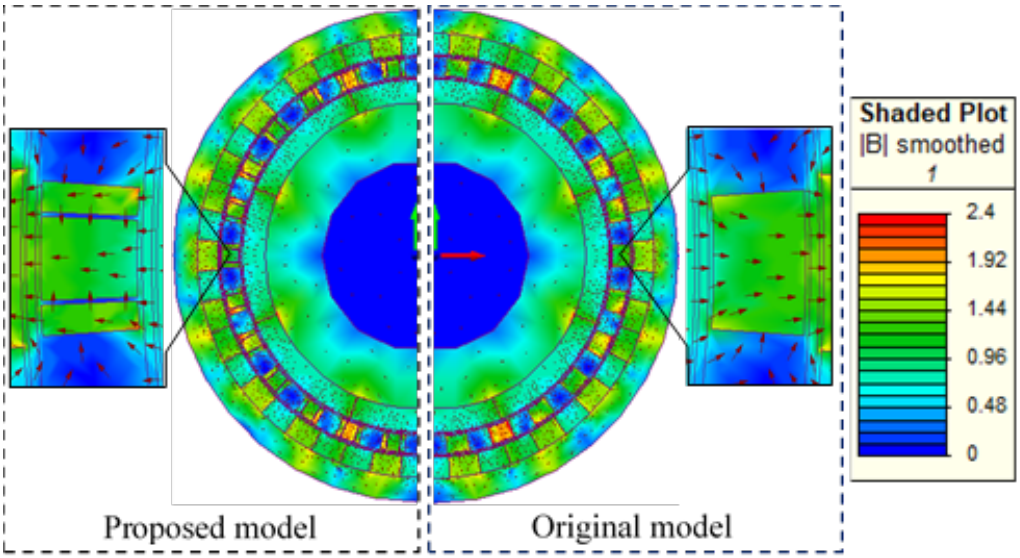

Fig. 8 Flux density distribution map of both models.

It is evident that the shape of the flux density waveform is unaffected by the proposed approach. Fig. 8 compares the flux density distribution map. Also, there are no saturation regions in the pole pieces meaning that this method does not affect the saturation level.

4.2 Cogging Torque Analysis

The preferable approach of determining the cogging torque is the static solver method, where the rotor is rotated in steps, and for each step, the cogging torque is determined taking into account that both rotors rotate synchronously by the gear ratio G_r. Fig. 9 illustrates the cogging torque variations with the slit angle, keeping the slit width d constant at d_o, viz. $T_{cog} = f(\alpha)$. It is clear that the optimal slit angle is 2.09^o through which least possible cogging torque is verified. The waveforms of cogging torque are plotted for one pole piece pitch, where 22 cycles of cogging torque are generated on both rotors. For the outer rotor, the cogging torque cycle is $0.6294\ ^o\ mech$. Conversely, the inner cogging torque cycle is $3.46\ ^o\ mech$. Fig. 10 compares the waveforms of cogging torque of the two models. The proposed approach significantly mitigated the cogging torque on the HSR. While on the LSR, there are 22 pole-pairs for which the LCM is 572; hence, the cogging torque of the original model has a small value, which after slitting, is slightly increased.

4.3 Torque Analysis

For maximum load angle (4.09^o) and optimal slit angle ($\alpha = 2.09^o$), the waveforms of the load torque of both rotors are depicted in Fig. 11. It is noticed that the mean torque values of the proposed model are less than those gained from the original model meaning that the proposed method causes small mitigation in the average torque. The FFT spectra of the torques (load and cogging torque) are shown in Fig. 12. Finally, Table 2 summarizes the results.

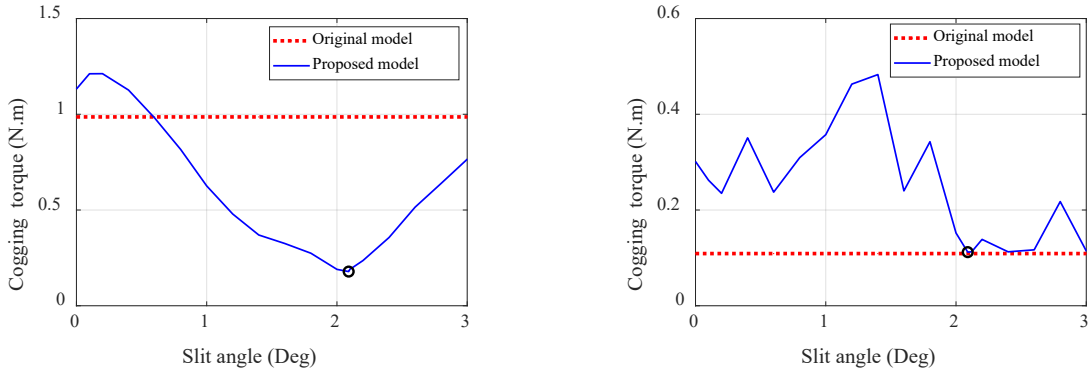

Fig. 9 Cogging torque variations with the slit angle for both rotors: a) HSR and b) LSR.

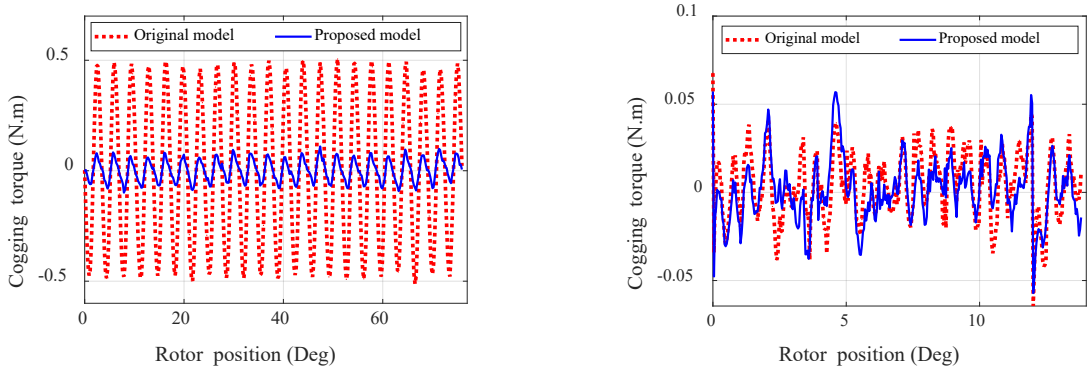

Fig. 10 Cogging torque waveforms of both rotors: a) HSR and b) LSR.

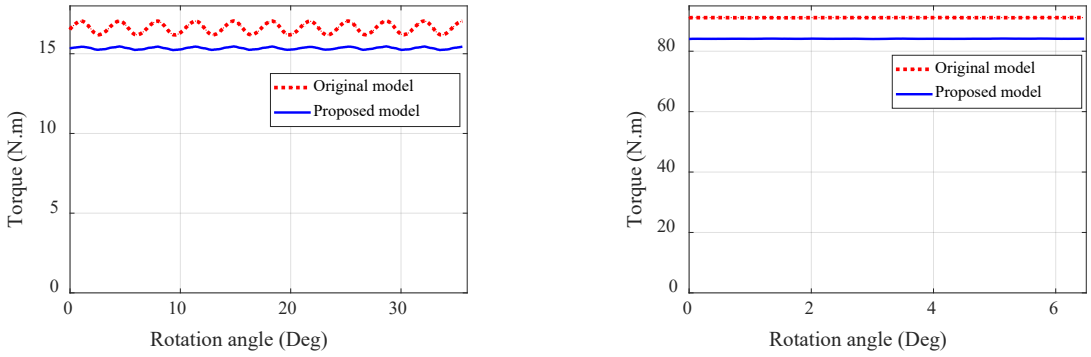

Fig. 11 Load torque waveforms of both rotors: a) HSR and b) LSR.

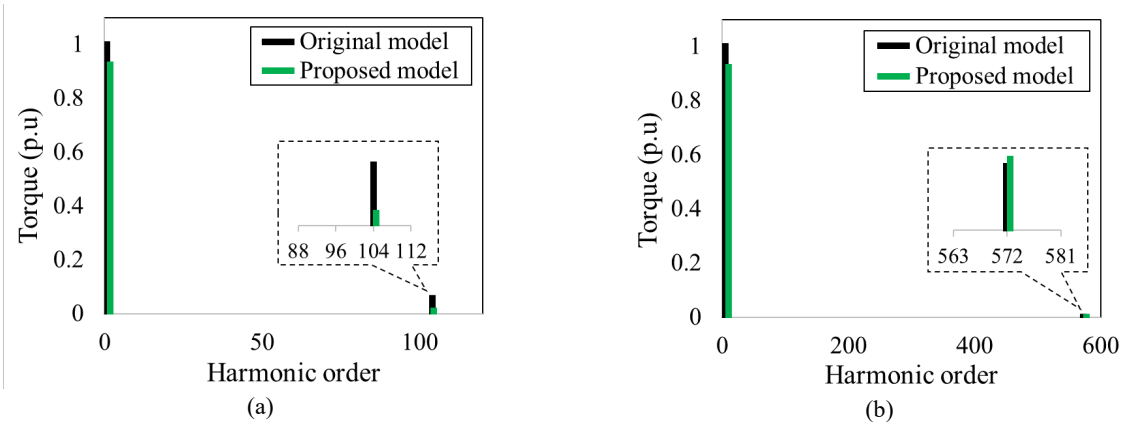

Fig. 12 FFT spectra of the load and cogging torque of both rotors: a) HSR and b) LSR.

Table 2 Summary of the results.

Description	Original MG	Proposed MG	Variation percentage (%)
HSR cogging torque, N.m	0.986	0.1785	81.9
LSR cogging torque, N.m	0.109	0.112	-2.75
HSR average torque, N.m	16.62	15.344	-7.68
LSR average torque, N.m	91.11	84.122	-7.67

5 Conclusion

In this research, an innovative, cost-effective approach for mitigating the cogging torque in MG has been proposed and compared with the original model. A comprehensive sensitivity analysis has been performed to evaluate this method. On this basis, the effect of the numbers, angles, and width of radial slits on the cogging torque mitigation had researched. The parameters n and α play a vital role in mitigating the cogging torque. The slitting method does not affect the shape of the flux density waveform in both rotors. Also, making a single slit on any side of the pole pieces mitigates the cogging torque regardless of its peaks oscillating around a non-zero value. Furthermore, bisecting the pole pieces with a single slit increases the cogging torque. It is found that the even number of slits gives promising results for which the cogging torque is dramatically mitigated. Moreover, the symmetrical slits of the pole pieces are recommended for mitigating the cogging torque. Therefore, by reasonably designing the ferromagnetic pole pieces, the cogging torque can appreciably be minimized, and the operation stability of the MG will be improved. The proposed technique is practical and can achieve low cogging torque in PM machines.

Intellectual Property

The authors confirm that they have given due consideration to the protection of intellectual property associated with this work and that there are no impediments to publication, including the timing to publication, with respect to intellectual property.

Funding

No funding was received for this work.

Credit Authorship Contribution Statement

M. K. Rashid: Research & Investigation**,** Data Curation**,** Analysis**,** Software and Simulation**,** Verification**,** Original Draft Preparation. **A. M. Mohammed:** Methodology, Project Administration**,** Software and Simulation**,** Supervision**,** Verification**,** Original Draft Preparation**,** Revise & Editing.

Declaration of Competing Interest

The authors hereby confirm that the submitted manuscript is an original work and has not been published so far, is not under consideration for publication by any other journal and will not be submitted to any other journal until the decision will be made by this journal. All authors have approved the manuscript and agree with its submission to “Iranian Journal of Electrical and Electronic Engineering”.

References

[1] X. Huang, Y. Guo, and L. Jing, "Comparative Analysis of Electromagnetic Performance of Magnetic Gear," *Progress In Electromagnetics Research Letters*, Vol. 97, pp. 69-76, 2021.

[2] C. C. Huang, M.C. Tsai, D. G. Dorrell, and B.J. Lin, "Development of a magnetic planetary gearbox," *IEEE Transactions on Magnetics*, Vol. 44, No. 3, pp. 403-412, 2008.

[3] L. Dosiek and P. Pillay, "Cogging torque reduction in permanent magnet machines," I*EEE Transactions on industry applications*, Vol. 43, No. 6, pp. 1565-1571, 2007.

[4] M. Jin, Y. Wang, J. Shen, P. Luk, W. Fei, and C. F. Wang, "Cogging torque suppression in a permanentmagnet flux-switching integrated-starter-generator," *IET Electric Power Applications*, , Vol. 4, pp. 647-656, 2010.

[5] X. Zhu, W. Hua, and Z. Wu, "Cogging torque minimization in flux-switching permanent magnet machines by right angle based tooth chamfering technique," *IET Electric Power Applications*, Vol. 12, 2017.

[6] H. C. Yu, H. W. Lai, L. J. Chen, and C. K. Lin, "Low cogging torque design and simplified model-free predictive current control for radial-flux dual three-phase permanent magnet electric machines," *Advances in Mechanical Engineering*, Vol. 11, No. 12, 2019.

[7] X. Zhu, W. Hua, and G. Zhang, "Analysis and reduction of cogging torque for flux-switching permanent magnet machines," *IEEE Transactions on Industry Applications*, Vol. 55, No. 6, pp. 5854-5864, 2019.

[8] V. Simón-Sempere, A. Simón-Gómez, M. Burgos-Payán, and J. R. Cerquides-Bueno, "Optimisation of Magnet Shape for Cogging Torque Reduction in Axial-Flux Permanent-Magnet Motors," *IEEE Transactions on Energy Conversion*, Vol. 36, No. 4, pp. 2825-2838, 2021.

[9] Y. Song, Z. Zhang, S. Yu, F. Zhang, and Y. Zhang, "Analysis and reduction of cogging torque in direct-drive external-rotor permanent magnet synchronous motor for belt conveyor application," I*ET Electric Power Applications*, Vol. 15, No. 6, pp. 668-680, 2021.

[10] T. Anuja and M. A. N. Doss, "Reduction of cogging torque in surface mounted permanent magnet brushless DC motor by adapting rotor magnetic displacement," *Energies*, Vol. 14, No. 10, p. 2861, 2021.

[11] Z. Zhu, Z. Azar, and G. Ombach, "Influence of additional air gaps between stator segments on cogging torque of permanent-magnet machines having modular stators," *IEEE Transactions on Magnetics*, Vol. 48, No. 6, pp. 2049-2055, 2011.

[12] L. Gašparin, A. Černigoj, and R. Fišer, "Additional cogging torque components due to asymmetry in stator back iron of PM synchronous motors," *COMPEL-The international journal for computation and mathematics in electrical and electronic engineering*, 2011.

[13] M. Nakano, Y. Morita, and T. Matsunaga, "Reduction of cogging torque due to production tolerances of rotor by using dummy slots placed partially in axial direction," *IEEE Transactions on Industry Applications*, Vol. 51, No. 6, pp. 4372-4382, 2015.

[14] A. Jabbari, "The Effect of Dummy Slots on Machine Performance in Brushless Permanent Magnet Machines: An Analytical, Numerical, and Experimental Study," *Iranian Journal of Electrical and Electronic Engineering*, Vol. 18, No. 2, pp. 2284-2284, 2022.

[15] Z. Zhu and D. Howe, "Influence of design parameters on cogging torque in permanent magnet machines," *IEEE Transactions on energy conversion*, Vol. 15, No. 4, pp. 407-412, 2000.

[16] S. M. Hwang, J. B. Eom, G. B. Hwang, W. B. Jeong, and Y. H. Jung, "Cogging torque and acoustic noise reduction in permanent magnet motors by teeth pairing," *IEEE Transactions on Magnetics*, Vol. 36, No. 5, pp. 3144-3146, 2000.

[17] Z. Zhu, J. Chen, L. Wu, and D. Howe, "Influence of stator asymmetry on cogging torque of permanent magnet brushless machines," I*EEE Transactions on Magnetics*, Vol. 44, No. 11, pp. 3851-3854, 2008.

[18] Z. Zhu, A. Thomas, J. Chen, and G. Jewell, "Cogging torque in flux-switching permanent magnet machines," *IEEE Transactions on Magnetics*, Vol. 45, No. 10, pp. 4708-4711, 2009.

[19] G. Li, B. Ren, Z. Zhu, Y. Li, and J. Ma, "Cogging torque mitigation of modular permanent magnet machines," *IEEE Transactions on Magnetics*, Vol. 52, No. 1, pp. 1-10, 2015.

[20] K. Atallah, S. D. Calverley, and D. Howe, "Design, analysis and realisation of a high-performance magnetic gear," *Electric Power Applications, IEE Proceedings*, Vol. 151, No. 2, pp. 135-143, 2004.

[21] D. C. Hanselman, Brushless permanent magnet motor design. *The Writers' Collective*, 2003.

M. K. Rashid was born in Dhi Qar, Iraq. He received the B.Sc. degree in 2014 from the University of Technology, Iraq in the field of electrical engineering. Currently, he is studying toward a Master's degree of Science in Electrical Engineering at the University of Technology, Iraq.

A. M. Mohammed received the B.Sc. and M.Sc. degrees from the University of Technology, Baghdad, Iraq, in 1995 and 2006, respectively, both in electrical and electronic engineering. He received the Ph.D. degree in electrical machines design in 2017 from the University of Nottingham, U.K. He is currently working as a lecturer in Electrical machines in the University of Technology, Iraq His research interests include high power electrical machines design, electromagnetic actuators and material characterization. He is also proficient in finite element

analysis.